

Coulomb dissociation of ${}^8\text{B}$ into ${}^7\text{Be} + p$: Effects of multiphoton exchange

S. Typel

Institut für Theoretische Physik I, Westfälische Wilhelms-Universität, Wilhelm-Klemm-Straße 9, D-48149 Münster, Germany

G. Baur

Institut für Kernphysik, Forschungszentrum Jülich GmbH, D-52425 Jülich, Germany

(Received 21 April 1994)

Coulomb dissociation of ${}^8\text{B}$ into the ${}^7\text{Be}$ - p low energy continuum is studied theoretically in first- and second-order perturbation theories and in the sudden approximation. The summation over all intermediate continuum states in the second-order amplitude is achieved by closure, using an expansion which is valid for low excitation energies. In view of the importance of the ${}^7\text{Be}(p,\gamma){}^8\text{B}$ reaction for the ${}^8\text{B}$ solar neutrino problem we investigate especially the optimal conditions for possible experiments. Double as well as triple differential cross sections are calculated for 5 MeV/ A , 46.5 MeV/ A , and 200 MeV/ A beam energy as a function of the ${}^8\text{B}^*$ scattering angle, the ${}^7\text{Be}$ - p relative energy, and momentum.

PACS number(s): 25.70.De, 25.40.Lw, 27.20.+n, 96.60.Kx

I. INTRODUCTION

The Coulomb dissociation approach has been suggested as an indirect method to obtain information about radiative capture reactions, relevant for nuclear astrophysics [1]. A few reactions have been studied so far, both experimentally and theoretically. A review was given recently [2]. Of particular interest is the radiative capture reaction ${}^7\text{Be}(p,\gamma){}^8\text{B}$, which is relevant for the ${}^8\text{B}$ solar neutrino problem. This is a key process in the high energy solar neutrino production through the ${}^8\text{B}$ β^+ decay (see, e.g., [3]).

A first attempt was made to study the ${}^8\text{B} \rightarrow {}^7\text{Be} + p$ Coulomb dissociation in the field of ${}^{208}\text{Pb}$ with a radioactive ${}^8\text{B}$ beam of 46.5 MeV/ A [4]. It is the aim of such kinds of experiments to obtain information on the astrophysical S factor for the ${}^7\text{Be}(p,\gamma){}^8\text{B}$ reaction. As is reviewed, e.g., in Ref. [2], there are various assumptions, which enter in such an analysis. One is the influence of nuclear excitation effects. This question was studied recently for this particular example, and the effects were found to be very small [5]. These effects are neglected in the present paper. We want to study the purely electromagnetic excitation effects of higher order for various kinematical conditions. Their knowledge will serve in optimizing future experiments. The difference between equivalent photon spectra of different multipolarity could also cause problems: Under the presently envisaged kinematical conditions we have $n_{E2} > n_{E1} > n_{M1}$. The $E2$ effects are expected to be disproportionally enhanced in the Coulomb dissociation process, whereas the $M1$ contribution, an effect of the order of about 10% in the relevant relative energy region, is suppressed in the Coulomb dissociation cross section, which leads to a lack of the corresponding information. This question is also under study presently [6–8].

The dominant effect is the $E1$ Coulomb dissociation into the $p + {}^7\text{Be}$ continuum. With the unequal charge-

to-mass ratio of the fragments p and ${}^7\text{Be}$ the effects of “post acceleration” could distort the information on the relative energy. In terms of purely classical ideas, one could imagine that the effects are rather conspicuous. It is the purpose of the present paper to give a quantum mechanical account of higher-order, or “post-acceleration” effects.

Two parameters serve to characterize electromagnetic excitation, the adiabaticity parameter ξ , which is defined by the ratio of the collision time to the nuclear transition period and the strength parameter χ (see, e.g., [9]). The adiabaticity parameter

$$\xi = \frac{(E_f - E_i)a}{\hbar v} \quad (1)$$

depends on the energy difference between initial and final states, half the distance at closest approach in a head-on collision, a , and the projectile velocity v . In the case of forward scattering the quantity [2]

$$\xi(\vartheta) = \frac{\xi}{2} \left(1 + \frac{1}{\sin(\vartheta/2)} \right) \quad (2)$$

with the scattering angle ϑ of the projectile is of interest. First-order theory is applicable for small χ and all $\xi(\vartheta)$, the sudden approximation for small $\xi(\vartheta)$ and all χ (Fig. 1). A recently developed method [10] for the calculation of second-order effects is a step into larger χ for values of $\xi(\vartheta)$, where the sudden approximation will no longer be a good approximation. Unfortunately, stepping further into the larger χ and $\xi(\vartheta)$ territory will lead to increasingly complex theoretical calculations. While this can be important for some aspects of the electromagnetic dissociation of very loosely bound systems, like ${}^{11}\text{Li}$ [11–13], the present method will be suitable for the ${}^8\text{B}$ case, where the penetration of the proton is reduced by the Coulomb barrier as compared to the neutrons in the ${}^{11}\text{Li}$ case.

In Sec. II we give the theoretical framework. We study

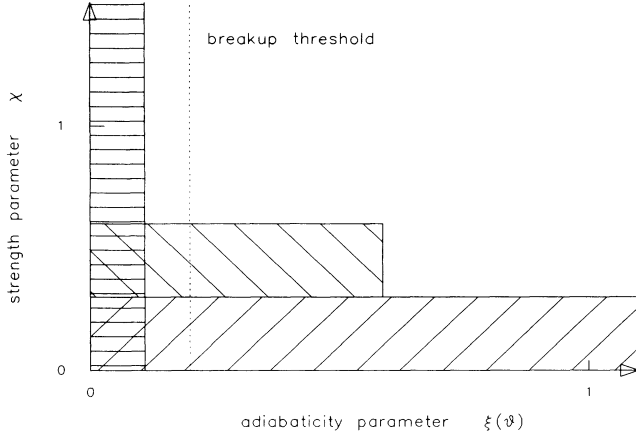


FIG. 1. The range of validity of the different approximations for the breakup amplitude is shown schematically. It depends on the strength parameter χ and the adiabaticity parameter $\xi(\vartheta)$. First-order (///) and second-order (\\\\) perturbation theories in the low ξ approach of Sec. II B, sudden approximation (\equiv).

higher-order effects in the sudden approximation, where all orders are taken into account, and in the new approach, where second-order effects are contained in the limit of small values of the adiabaticity parameter. Using the nuclear model of ^8B as given in Sec. III for the direct capture calculation, this theory is applied in Sec. IV to the case of ^8B Coulomb dissociation at various projectile energies. The electromagnetic excitation is determined by electromagnetic matrix elements between the nuclear states. If the “no penetration condition” holds [2] these are taken at the “photon point.” Since we treat higher-order effects by closure, new types of nuclear matrix-elements [see, e.g., Eq. (12) below] appear. We evaluate them here in realistic models. However, this model dependence will not lead to ambiguities in our conclusions, which are given in Sec. V.

II. THEORETICAL TREATMENT OF HIGHER-ORDER ELECTROMAGNETIC EXCITATION INTO THE CONTINUUM

Typically we study the medium energy light ion dissociation on heavy nuclei. The semiclassical method, where the c.m. motion of the projectile is treated classically, is well applicable. On the other hand, it seems indispensable to treat the projectile system in a fully quantal way. This is already evident from the fact that only low partial waves, $l = 0, 1$, or 2 , say, are involved. There is no classical analogue and the concepts of breakup radius, initial breakup configurations, from where a classical trajectory calculation is started, are, at best, rather vague. No quantitative conclusion can be drawn from such calculations. In order to fix notation, we review in Sec. II A the formulas for first-order excitation. Following the development of Ref. [10], we give in detail the second-order formulas in Sec. II B. In Sec. II C we give the formulas

for the sudden approximation.

The ground state $|i\rangle$ of the projectile is excited to the final state $|f\rangle$ by the external time-dependent perturbation

$$H(t) = \int d^3r \left(\frac{Ze}{|\mathbf{r} - \mathbf{R}(t)|} - \frac{Ze}{|\mathbf{R}(t)|} \right) \times \left(\rho(\mathbf{r}) - \frac{1}{c^2} \mathbf{j}(\mathbf{r}) \cdot \dot{\mathbf{R}}(t) \right), \quad (3)$$

where $\rho(\mathbf{r})$ is the charge density operator, $\mathbf{j}(\mathbf{r})$ is the current density operator, and $\mathbf{R}(t)$ gives the time-dependent position of the target with charge number Z in the projectile frame. From the excitation amplitude a_{fi} , which is given in the various approximations below, we get the triple differential cross section from

$$\frac{d^3\sigma}{dE d\Omega_k d\Omega_q} = \frac{d\sigma_R}{d\Omega_k} \frac{1}{2J_i + 1} \sum_{M_i m_i} |a_{fi}|^2 \frac{\mu_{bc} q}{(2\pi)^3 \hbar^2} \quad (4)$$

for the excitation of the ground state with angular momentum J_i to the final state with spin I , relative momentum $\hbar\mathbf{q}$, and energy E between the two fragments b and c with reduced mass μ_{bc} . The Rutherford cross section $\frac{d\sigma_R}{d\Omega_k}$ is calculated for the scattering of the center of mass of the projectile in the direction $\hbar\mathbf{k}$. The angular correlation of the fragments [Eq. (4)] can be expressed as a sum over contributions from different spherical harmonics depending on the direction of $\hbar\mathbf{q}$ [14]. An integration over these directions yields the double differential cross sections in which the contributions of different multipolarity are summed up incoherently.

A. First-order electromagnetic excitation

In perturbation theory the full excitation amplitude is given as a sum

$$a_{fi} = \delta_{fi} + a_{fi}^{(1)} + a_{fi}^{(2)} + \dots \quad (5)$$

of contributions of different order. The first-order amplitude

$$a_{fi}^{(1)} = \frac{1}{i\hbar} \langle f | \int_{-\infty}^{\infty} dt e^{i\omega t} H(t) | 0 \rangle \quad (6)$$

with $\omega = (E_f - E_i)/\hbar$ is calculated in a standard way by expanding the perturbation $H(t)$ in multipoles

$$a_{fi}^{(1)} = 4\pi \frac{Ze}{i\hbar} \sum_{\lambda\mu} \frac{(-1)^\mu}{2\lambda + 1} \langle f | \mathcal{M}(\pi\lambda - \mu) | i \rangle S_{\pi\lambda\mu}(\omega) \quad (7)$$

with the usual electric ($\pi = E$) and magnetic ($\pi = M$) multipole operators $\mathcal{M}(\pi\lambda\mu)$, the electric orbital integrals

$$S_{E\lambda\mu}(\omega) = \int_{-\infty}^{\infty} dt \frac{e^{i\omega t}}{R(t)^{\lambda+1}} Y_{\lambda\mu}(\hat{\mathbf{R}}(t)), \quad (8)$$

and the magnetic orbital integrals

$$S_{M\lambda\mu}(\omega) = \frac{i}{c\lambda} \int_{-\infty}^{\infty} dt \frac{e^{i\omega t}}{R(t)^{\lambda+1}} \dot{\mathbf{R}}(t) \cdot \hat{\mathbf{L}} Y_{\lambda\mu}(\hat{\mathbf{R}}(t)) \quad (9)$$

with $\hat{\mathbf{L}} = -i\mathbf{R} \times \nabla_{\mathbf{R}}$. For relativistic corrections at higher projectile energies see [15].

B. Second-order electromagnetic excitation for small adiabaticity parameters

The second-order contribution to the excitation amplitude in the perturbation expansion is given by

$$a_{fi}^{(2)} = \frac{1}{(i\hbar)^2} \langle f | \int_{-\infty}^{\infty} dt \int_{-\infty}^t dt' e^{\frac{iH_0 t}{\hbar}} H(t) e^{-\frac{iH_0 t}{\hbar}} e^{\frac{iH_0 t'}{\hbar}} \times H(t') e^{-\frac{iH_0 t'}{\hbar}} | i \rangle, \quad (10)$$

where H_0 is the Hamiltonian of the projectile system. In the limit of fast collisions this can be approximated by [10]

$$a_{fi}^{(2)} = \frac{1}{(i\hbar)^2} \langle f | \int_{-\infty}^{\infty} dt \int_{-\infty}^t dt' \theta(t-t') e^{i\omega(t+t')} \left\{ H(t)H(t') - \frac{it'}{\hbar} [H_0, H(t)]H(t') - \frac{it}{\hbar} H(t)[H_0, H(t')] \right\} | i \rangle \quad (11)$$

with $\theta(t-t') = 1(0)$ if $t > t'$ ($t < t'$). The multipole expansion of the perturbation leads to

$$a_{fi}^{(2)} = \left(4\pi \frac{Ze}{i\hbar} \right)^2 \sum_{\substack{\pi_1 \lambda_1 \mu_1 \\ \pi_2 \lambda_2 \mu_2}} \frac{(-1)^{\mu_1 + \mu_2}}{(2\lambda_1 + 1)(2\lambda_2 + 1)} \left\{ \langle f | \mathcal{M}(\pi_1 \lambda_1 - \mu_1) \mathcal{M}(\pi_2 \lambda_2 - \mu_2) | i \rangle Q(S_{\pi_1 \lambda_1 \mu_1}(\omega) S_{\pi_2 \lambda_2 \mu_2}(\omega)) \right. \\ \left. + \frac{a}{v\hbar} \langle f | [H_0, \mathcal{M}(\pi_1 \lambda_1 - \mu_1)] \mathcal{M}(\pi_2 \lambda_2 - \mu_2) | i \rangle Q(S_{\pi_1 \lambda_1 \mu_1}(\omega) R_{\pi_2 \lambda_2 \mu_2}(\omega)) \right. \\ \left. + \frac{a}{v\hbar} \langle f | \mathcal{M}(\pi_1 \lambda_1 - \mu_1) [H_0, \mathcal{M}(\pi_2 \lambda_2 - \mu_2)] | i \rangle Q(R_{\pi_1 \lambda_1 \mu_1}(\omega) S_{\pi_2 \lambda_2 \mu_2}(\omega)) \right\}, \quad (12)$$

where new types of nuclear matrix-elements appear. Here we introduce the modified electric orbital integrals

$$R_{E\lambda\mu}(\omega) = -i \frac{v}{a} \int_{-\infty}^{\infty} dt \frac{te^{i\omega t}}{R(t)^{\lambda+1}} Y_{\lambda\mu}(\hat{\mathbf{R}}(t)), \quad (13)$$

the modified magnetic orbital integrals

$$R_{M\lambda\mu}(\omega) = \frac{1}{a\lambda} \frac{v}{c} \int_{-\infty}^{\infty} dt \frac{te^{i\omega t}}{R(t)^{\lambda+1}} \dot{\mathbf{R}}(t) \cdot \hat{\mathbf{L}} Y_{\lambda\mu}(\hat{\mathbf{R}}(t)), \quad (14)$$

and the abbreviation

$$Qf(\omega_1, \omega_2) = \frac{1}{2} f(\omega_1, \omega_2) + \frac{i}{2\pi} \mathcal{P} \int_{-\infty}^{\infty} \frac{dq}{q} f(\omega_1 - q, \omega_2 + q). \quad (15)$$

We define the functions

$$T_{\lambda\mu}^{\pi_1 \lambda_1 \pi_2 \lambda_2}(\omega_1, \omega_2) = \sum_{\mu_1 \mu_2} (\lambda_1 \mu_1 \lambda_2 \mu_2 | \lambda \mu) S_{\pi_1 \lambda_1 \mu_1}(\omega_1) S_{\pi_2 \lambda_2 \mu_2}(\omega_2), \quad (16)$$

$$U_{\lambda\mu}^{\pi_1 \lambda_1 \pi_2 \lambda_2}(\omega_1, \omega_2) = \sum_{\mu_1 \mu_2} (\lambda_1 \mu_1 \lambda_2 \mu_2 | \lambda \mu) S_{\pi_1 \lambda_1 \mu_1}(\omega_1) R_{\pi_2 \lambda_2 \mu_2}(\omega_2), \quad (17)$$

$$V_{\lambda\mu}^{\pi_1 \lambda_1 \pi_2 \lambda_2}(\omega_1, \omega_2) = \sum_{\mu_1 \mu_2} (\lambda_1 \mu_1 \lambda_2 \mu_2 | \lambda \mu) R_{\pi_1 \lambda_1 \mu_1}(\omega_1) S_{\pi_2 \lambda_2 \mu_2}(\omega_2), \quad (18)$$

by angular momentum coupling with the symmetry properties

$$T_{\lambda\mu}^{\pi_1 \lambda_1 \pi_2 \lambda_2}(\omega_1, \omega_2) = (-1)^{\lambda_1 + \lambda_2 - \lambda} T_{\lambda\mu}^{\pi_2 \lambda_2 \pi_1 \lambda_1}(\omega_2, \omega_1), \quad (19)$$

$$U_{\lambda\mu}^{\pi_1 \lambda_1 \pi_2 \lambda_2}(\omega_1, \omega_2) = (-1)^{\lambda_1 + \lambda_2 - \lambda} V_{\lambda\mu}^{\pi_2 \lambda_2 \pi_1 \lambda_1}(\omega_2, \omega_1), \quad (20)$$

and the new multipole operators

$$\mathcal{N}_{\pi_1\pi_2}^{\lambda_1\lambda_2}(\lambda-\mu) = \sum_{\mu_1\mu_2} (\lambda_1\mu_1\lambda_2\mu_2|\lambda\mu) \mathcal{M}(\pi_1\lambda_1 - \mu_1) \mathcal{M}(\pi_2\lambda_2 - \mu_2), \quad (21)$$

$$\mathcal{K}_{\pi_1\pi_2}^{\lambda_1\lambda_2}(\lambda-\mu) = \sum_{\mu_1\mu_2} (\lambda_1\mu_1\lambda_2\mu_2|\lambda\mu) \mathcal{M}(\pi_1\lambda_1 - \mu_1) H_0 \mathcal{M}(\pi_2\lambda_2 - \mu_2). \quad (22)$$

With these definitions the second-order amplitude becomes

$$\begin{aligned} a_{fi}^{(2)} = & \left(4\pi \frac{Ze}{i\hbar}\right)^2 \sum_{\substack{\pi_1\lambda_1\pi_2\lambda_2 \\ \lambda\mu}} \frac{(-1)^\mu}{(2\lambda_1+1)(2\lambda_2+1)} \\ & \times \left\{ \langle f | \mathcal{N}_{\pi_1\pi_2}^{\lambda_1\lambda_2}(\lambda-\mu) | i \rangle \left(QT_{\lambda\mu}^{\pi_1\lambda_1\pi_2\lambda_2}(\omega, \omega) + \frac{aE_f}{v\hbar} QU_{\lambda\mu}^{\pi_1\lambda_1\pi_2\lambda_2}(\omega, \omega) - \frac{aE_i}{v\hbar} QV_{\lambda\mu}^{\pi_1\lambda_1\pi_2\lambda_2}(\omega, \omega) \right) \right. \\ & \left. - \frac{a}{v\hbar} \langle f | \mathcal{K}_{\pi_1\pi_2}^{\lambda_1\lambda_2}(\lambda-\mu) | i \rangle \left(QU_{\lambda\mu}^{\pi_1\lambda_1\pi_2\lambda_2}(\omega, \omega) - QV_{\lambda\mu}^{\pi_1\lambda_1\pi_2\lambda_2}(\omega, \omega) \right) \right\}. \quad (23) \end{aligned}$$

This expression can be simplified by using the symmetry relations and choosing the energy scale so that $E_i + E_f = 0$. In the special case where we restrict ourselves to, e.g., only one electric multipole ($\lambda' = \lambda_1 = \lambda_2$) we get for even $2\lambda' - \lambda$

$$\begin{aligned} a_{fi}^{(2)} = & \left(4\pi \frac{Ze}{i\hbar}\right)^2 \sum_{\mu} \frac{(-1)^\mu}{(2\lambda'+1)^2} \left\{ \frac{1}{2} \langle f | \mathcal{N}_{EE}^{\lambda'\lambda'}(\lambda-\mu) | i \rangle \left(T_{\lambda\mu}^{E\lambda'E\lambda'}(\omega, \omega) + \xi U_{\lambda\mu}^{E\lambda'E\lambda'}(\omega, \omega) \right) \right. \\ & \left. - \frac{a}{v\hbar} \langle f | \mathcal{K}_{EE}^{\lambda'\lambda'}(\lambda-\mu) | i \rangle \frac{i}{\pi} \mathcal{P} \int_{-\infty}^{\infty} \frac{dq}{q} U_{\lambda\mu}^{E\lambda'E\lambda'}(\omega - q, \omega + q) \right\} \quad (24) \end{aligned}$$

with the adiabaticity parameter ξ [Eq. (1)]. In the limit of vanishing ξ we will remain with

$$a_{fi}^{(2)} = \frac{1}{2} \left(4\pi \frac{Ze}{i\hbar}\right)^2 \sum_{\mu} \frac{(-1)^\mu}{(2\lambda'+1)^2} \langle f | \mathcal{N}_{EE}^{\lambda'\lambda'}(\lambda-\mu) | i \rangle T_{\lambda\mu}^{E\lambda'E\lambda'}(0, 0) \quad (25)$$

as is expected from the expansion of the amplitude in sudden approximation to second order.

C. Sudden approximation

The excitation amplitude in sudden approximation is given by

$$a_{fi}^{sa} = \langle f | \exp \left(\frac{1}{i\hbar} \int_{-\infty}^{\infty} dt H(t) \right) | i \rangle. \quad (26)$$

It takes all orders of the interaction into account but is only valid if the time ordering can be neglected, i.e., for small $\xi(\vartheta)$. The amplitude can be expanded into a sum of contributions of different multipolarity

$$a_{fi}^{sa} = 4\pi \frac{Ze}{i\hbar} \sum_{\lambda\mu} \frac{(-1)^\mu}{2\lambda+1} \langle f | \omega_{\lambda-\mu}^{sa}(r) Y_{\lambda-\mu}(\hat{\mathbf{r}}) | i \rangle \quad (27)$$

like the first-order amplitude [Eq. (7)] by defining the radial operators

$$\begin{aligned} \omega_{\lambda-\mu}^{sa}(r) = & \frac{i\hbar(2\lambda+1)}{4\pi Ze} \\ & \times \int d\Omega_r \left[\exp \left(\frac{1}{i\hbar} \int_{-\infty}^{\infty} dt H(t) \right) - 1 \right] Y_{\lambda\mu}(\hat{\mathbf{r}}) \quad (28) \end{aligned}$$

through angular integration over the directions of the relative coordinate $\mathbf{r} = \mathbf{r}_b - \mathbf{r}_c$ between the fragments. These operators differ in their radial dependence from the usual electromagnetic multipole operators, especially at large r . Considering only electric excitations the argument of the exponential function can be expressed as

$$\frac{1}{i\hbar} \int_{-\infty}^{\infty} dt H(t) = 4\pi \frac{Ze}{i\hbar} \sum_{\lambda\mu} \frac{Z_{\text{eff}}^{(\lambda)} e}{2\lambda+1} r^\lambda Y_{\lambda\mu}^*(\hat{\mathbf{r}}) S_{E\lambda\mu}(0). \quad (29)$$

The orbital integrals $S_{E\lambda\mu}(0)$ can be calculated analytically. The effective charge number is given by

$$Z_{\text{eff}}^{(\lambda)} = Z_b \left(\frac{m_c}{m_b + m_c} \right)^\lambda + Z_c \left(\frac{-m_b}{m_b + m_c} \right)^\lambda \quad (30)$$

with the charge numbers Z_b and Z_c and the masses m_b and m_c of the fragments. Even if only a small number of multipoles in the sum is considered the action of the exponential function will produce all kinds of multipole contributions representing the higher-order effects.

III. DIRECT CAPTURE MODEL

We describe the ${}^8\text{B}$ system in a ${}^7\text{Be}$ - p cluster model, where the relative wave functions for the bound and scattering states are generated from simple Woods-Saxon potentials. The ${}^7\text{Be}$ nucleus is assumed to be in the ground state with angular momentum $j = \frac{3}{2}$, which is coupled with the spin of the proton to the channel spin $I = 2$. In this approach we have neglected contributions of channel spin 1, which is also possible in principle. The orbital angular momentum of the relative motion is then coupled with the channel spin to the total angular momentum and parity J^π of the ground and the scattering states. The bound state of ${}^8\text{B}$ with total angular momentum 2^+ is described as a p wave while for the scattering states we use s , p , and d waves, which will be sufficient at small relative energies E . The ${}^7\text{Be}$ - p potential is given by

$$V = V_C(r) + V_{LS}(r) \frac{\mathbf{L} \cdot \mathbf{S}}{\hbar^2} \quad (31)$$

with a central and a spin-orbit part. They have a common shape ($x = C$, respectively, LS)

$$V_x(r) = -V_x^L \left[1 + \exp \left(\frac{r - R}{a} \right) \right]^{-1} \quad (32)$$

but different depths depending on the relative orbital angular momentum L . The parameters of the potential are chosen starting from the set of Barker [16] with $R = 2.95$ fm and $a = 0.65$ fm for the radius and diffuseness parameter. For the wave functions with $L = 0$, respectively, $L = 2$ the central depths are taken to be $V_C^0 = 56.18$ MeV, respectively, $V_C^2 = 50$ MeV. The spin-orbit part is only used for the p -wave states. We choose $V_C^1 = 48.07$ MeV and $V_{LS}^1 = 1.51$ MeV to reproduce the binding energy of ${}^8\text{B}$ ($E_B = 137.4$ keV, referring to the ${}^7\text{Be}$ - p breakup threshold) and the resonance energy of the 1^+ state ($E = 633$ keV). The radial wave function of the bound state is matched asymptotically to a Whittaker function, and the matrix elements of the electric multipole operators are calculated without using the long wavelength approximation. The radial integration is carried out up to 300 fm because of the far reaching integrand.

The ground state of ${}^8\text{B}$ and the s - and d -wave scattering states are sufficiently well described in our model to give an astrophysical S factor for the $E1$ direct capture reaction similar to earlier and more elaborate calculations [16–20]. The result also agrees with the low-energy direct capture measurements of the S factor within the experimental uncertainties (Fig. 2). The $E2$ contributions to the capture cross section can be neglected at small energies (Fig. 3). We get a resonant quadrupole contribution only from the 1^+ state but not from the p -wave states with other total angular momenta. Our

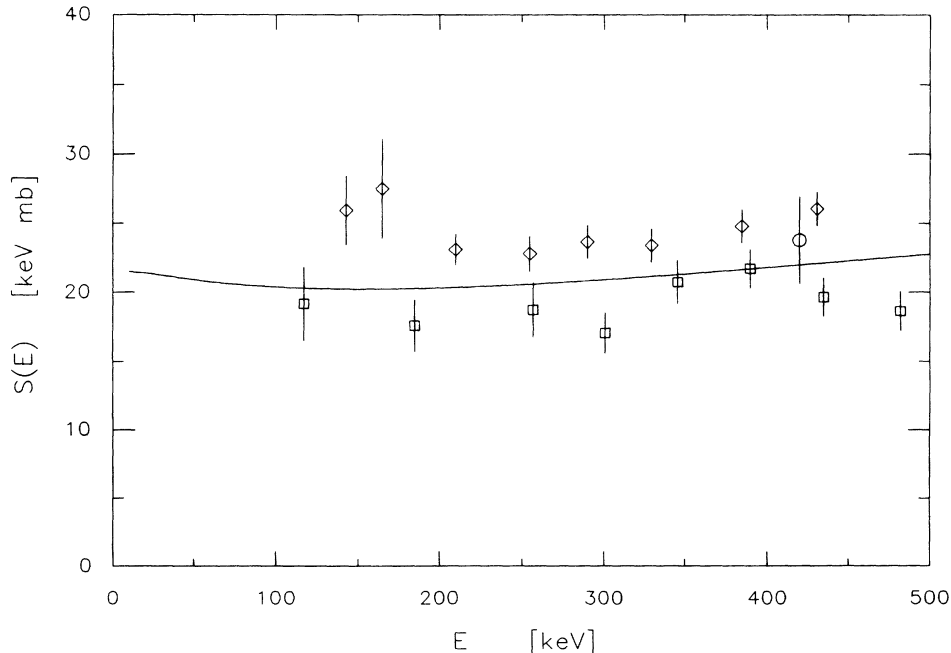


FIG. 2. S factor of the ${}^7\text{Be}(p,\gamma){}^8\text{B}$ reaction for the $E1$ capture from s and d waves to the p -wave ground state. Experimental data: Parker *et al.* (\circ , [24]), Kavanagh *et al.* (\diamond , [25]), Filippone *et al.* (\square , [26]).

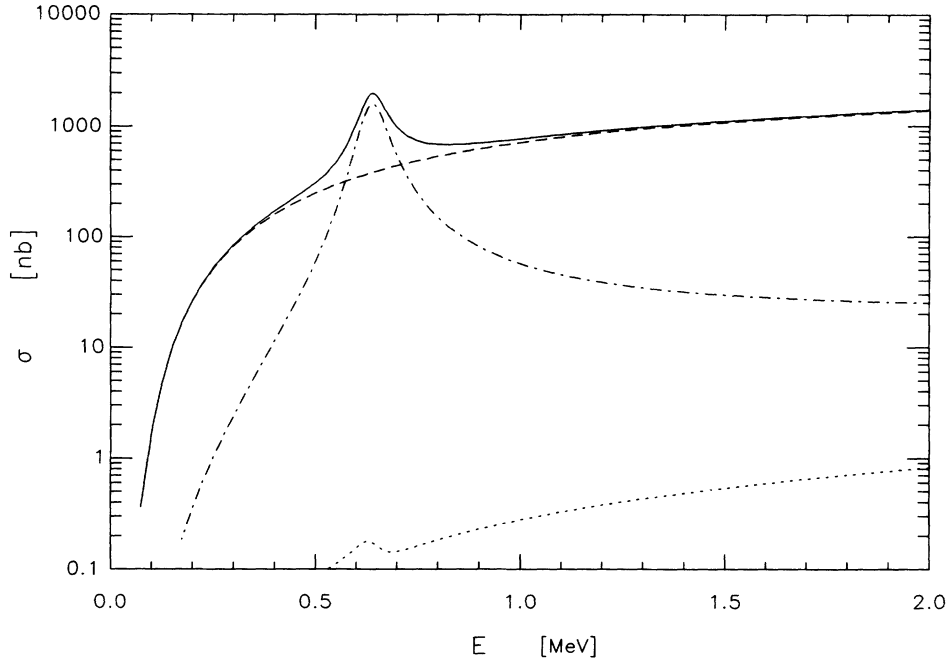


FIG. 3. Capture cross section of the ${}^7\text{Be}(p,\gamma){}^8\text{B}$ reaction (solid line) with multipole contributions from $E1$ (dashed line), $E2$ (dotted line) and $M1$ (dashed-dotted line).

$E2$ contribution is smaller than in the studies which are carried out in Refs. [17,19,20]. This behavior is caused by the use of a different potential and the neglect of the f -wave contributions in our calculation. At the resonance we have to consider the $M1$ contribution to the cross section. The actual structure of the 1^+ resonance in ${}^8\text{B}$ is quite different from our simple ${}^7\text{Be}-p$ cluster model. We get a resonance width of 78 keV, about twice the experimental value of (37 ± 5) keV [21]. The radial wave functions of the ground state and the resonance are almost orthogonal, resulting in a strong suppression of the $M1$ contribution [19]. Therefore we have to scale the $M1$ contribution to the capture cross section to give approximately the experimental magnitude. This was done by multiplying the reduced matrix elements with the factor 15. The scaling is appropriate in the resonance region. In the continuum region we will get a too large spurious $M1$ contribution, hence we neglect it in the S factor (Fig. 2). This defect in our calculation will, however, not affect the conclusions where the Coulomb dissociation is concerned, since only the model-independent reduced transition probability $B(M1)$ enters and the $M1$ contribution to the breakup will be important only in the resonance region.

Our model for the ${}^7\text{Be}(p,\gamma){}^8\text{B}$ reaction is only a test model, which cannot give precise quantitative results of all aspects of the process. Especially the $E2$ and $M1$ contributions might be considerably different in a better theoretical description of the reaction. But the simple model allows us to study the qualitative features of the Coulomb dissociation as compared to the radiative capture reaction.

IV. COULOMB DISSOCIATION

Using the wave functions and electromagnetic multipole matrix elements as calculated in the direct capture model we will now examine in detail the breakup reaction ${}^8\text{B} + {}^{208}\text{Pb} \rightarrow {}^7\text{Be} + p + {}^{208}\text{Pb}$. In order to reveal the physics of the process, we give here results for different values of various parameters (incident energy, ${}^8\text{B}^*$ scattering angle, and ${}^8\text{B}$ excitation energy). The calculation includes relativistic corrections as given in [15]. First-order cross sections contain $E1$, $E2$, and $M1$ contributions. The second-order amplitude in our model gets monopole and quadrupole contributions from $E1E1$ and $E2E2$ couplings. Additionally there are dipole contributions from the $E1E2$ coupling. Second-order contributions from $M1$ couplings are neglected because they are expected to be very small in the continuum region. The amplitude in sudden approximation is calculated including electric dipole and quadrupole contributions in the argument [Eq. (29)] of the exponential function, which leads to the relevant monopole, dipole and quadrupole operators. We neglect the magnetic contribution in the sudden approximation. The terms with the operator $\mathcal{K}_{\pi_1\pi_2}^{\lambda_1\lambda_2}(\lambda - \mu)$ in the second-order amplitude [Eq. (23)] are neglected because of their smallness. In the long wavelength limit the first-order electric quadrupole operator and the second-order quadrupole operator from the $E1E1$ coupling have the same \mathbf{r} dependence. The ratio of the corresponding amplitudes is therefore independent of the radial and angular integrals. In the limit $\xi \rightarrow 0$ we get for the ratio of the corresponding cross sections

$$\frac{d^2\sigma}{dEd\Omega_k}(E1E1 \rightarrow E2, 2^{nd}) \bigg/ \frac{d^2\sigma}{dEd\Omega_k}(E2, 1^{st}) = \frac{4}{3}(Z\alpha)^2 \left(\frac{c}{v}\right)^2 \frac{(Z_{\text{eff}}^{(1)})^4}{(Z_{\text{eff}}^{(2)})^2}, \quad (33)$$

with the electromagnetic fine structure constant $\alpha \approx \frac{1}{137}$. In general we have $Z_{\text{eff}}^{(1)} \ll Z_{\text{eff}}^{(2)}$ [Eq. (30)]. Higher-order effects can show up strongly in the scattering on highly charged targets at small projectile velocities. Similar expressions for the cross sections can be obtained by com-

paring the radial dependences of other second-order operators with electric operators of higher multipolarity.

First experiments were carried out with a ^8B secondary beam of 46.5 MeV/A at RIKEN [4]. Figure 4 shows our numerical results at this incident energy for the double

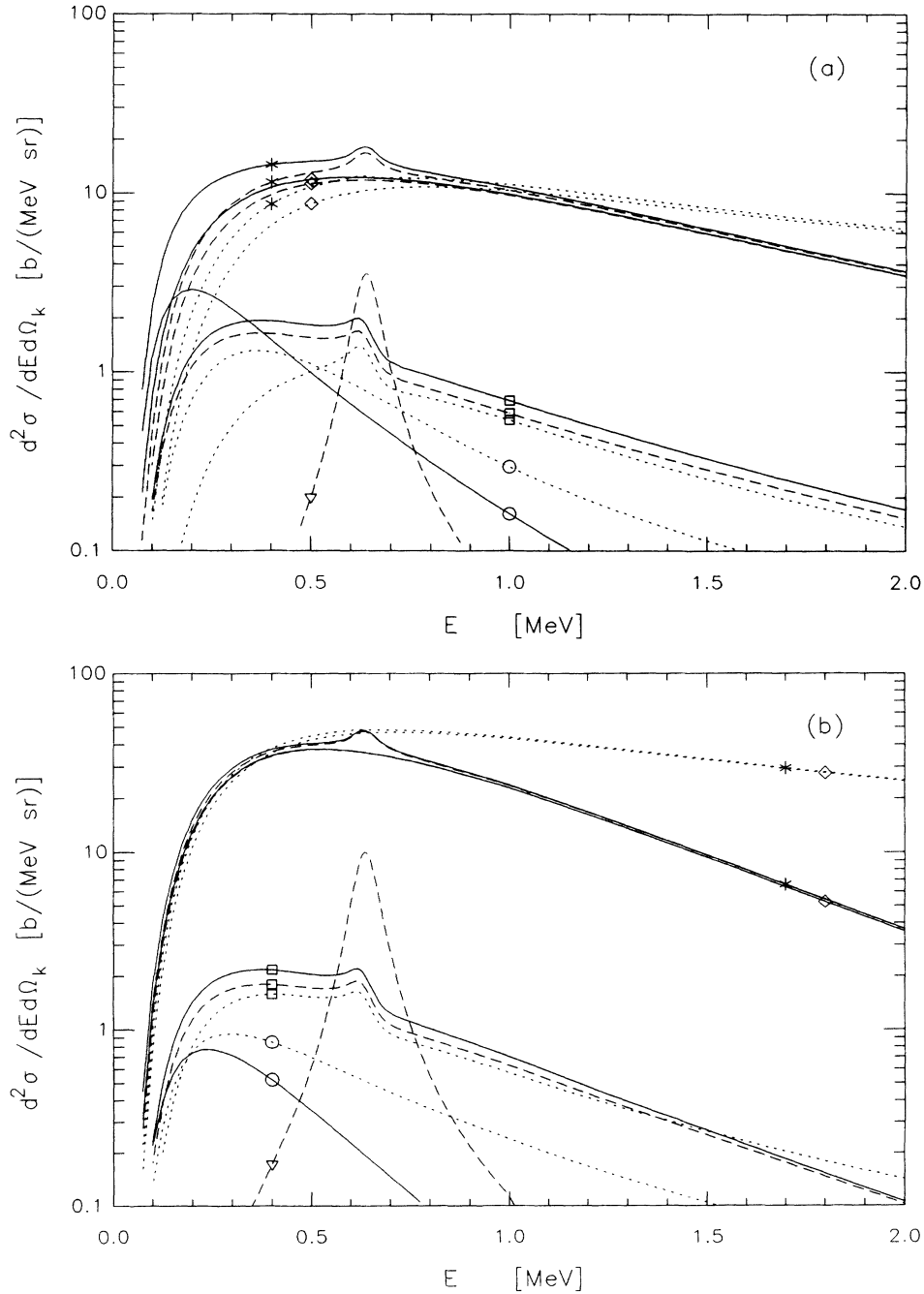


FIG. 4. Breakup cross section of the reaction $^8\text{B} + ^{208}\text{Pb} \rightarrow ^7\text{Be} + p + ^{208}\text{Pb}$ as a function of the relative energy E for a ^8B scattering angle of (a) $\vartheta = 3^\circ$, (b) $\vartheta = 1.5^\circ$, and a projectile energy of 46.5 MeV/A. First order (dashed line), first + second order (solid line) calculation, sudden approximation (dotted line). Electric monopole (\circ), dipole (\diamond), quadrupole (\square), magnetic dipole (∇), total ($*$).

differential cross section as a function of the relative energy E of the fragments. We choose scattering angles corresponding to impact parameters, which are typical for the RIKEN experiment. The first-order $M1$ excitation is very small, as expected due to a $(\frac{v}{c})^2$ factor. The first-order $E2$ contribution relative to the $E1$ contribution is strongly enhanced as compared to the $E2/E1$ ratio in the capture cross section as was noticed earlier [6]. For small ξ this ratio can be approximated by $4/(k_\gamma b)^2$ [2] with the momentum $\hbar k_\gamma$ of the exchanged photon and the impact parameter b . Higher-order effects are important at small breakup energies and decrease at higher energies. The $E1E1$, $E1E2$, and $E2E2$ couplings in the second-order amplitude change the electric dipole and quadrupole contributions to the breakup cross section and cause an electric monopole contribution. We did not include the couplings with the magnetic dipole transition in the second-order amplitude because the change of the total breakup cross section in the continuum region is negligible but in the used nuclear model it would be overestimated. At a larger impact parameter, i.e., smaller scattering angle, higher-order contributions become rather small and first-order $E1$ excitation clearly dominates.

The sudden approximation overestimates the cross section at higher relative energies and small scattering angles as the interaction becomes adiabatic. At very small excitation energies it tends to be smaller than the results from the first- and second-order perturbation theories. This can be understood from the r dependence of the multipole operators in the radial integral. In the limit $\xi \rightarrow 0$, i.e., the long wavelength approximation, the usual multipole operators rise like a power of r , and the essential contributions in the integral are far outside the

nucleus for a system like ^8B with a small binding energy. The radial operators in the sudden approximation [Eq. (28)] show an oscillatory behavior like Bessel functions because of the finite strength parameter. So even for moderately small values of χ they will attain a maximum at rather small distances of the fragments, and the integrand will decrease faster. More tightly bound systems will be much less sensitive to higher-order effects as the main contributions are confined to the range of the nucleus. This effect must be taken more care of in the future.

There are ideas [22] to study the ^8B dissociation at energies below the Coulomb barrier. Since the binding energy of ^8B is more than a factor 10 lower as compared to the deuteron, this seems a point worthy of study. (For a review of deuteron breakup, see, e.g., [23]. In this case, the post-form DWBA leads to a good description of the process. This may be even qualitatively different for the case of the extremely loosely bound ^8B .) We look at the excitation cross section at a projectile energy of 5 MeV/A and a scattering angle of 15° (Fig. 5). Higher-order effects become very important in the interesting region of small relative energy. At increasing relative energies the total cross section vanishes rapidly and higher-order effects are unimportant. The sudden approximation is not really applicable, in general, even very close to the breakup threshold as the adiabaticity parameter is always larger than $\xi(\vartheta) \approx 0.22$. The study of the ^8B sub-Coulomb breakup shows very interesting features, in some contrast to the much more tightly bound deuteron.

In Fig. 6 we look at the dependence of the breakup cross section on the scattering angle for a fixed relative energy of the fragments. The maximum in the cross sec-

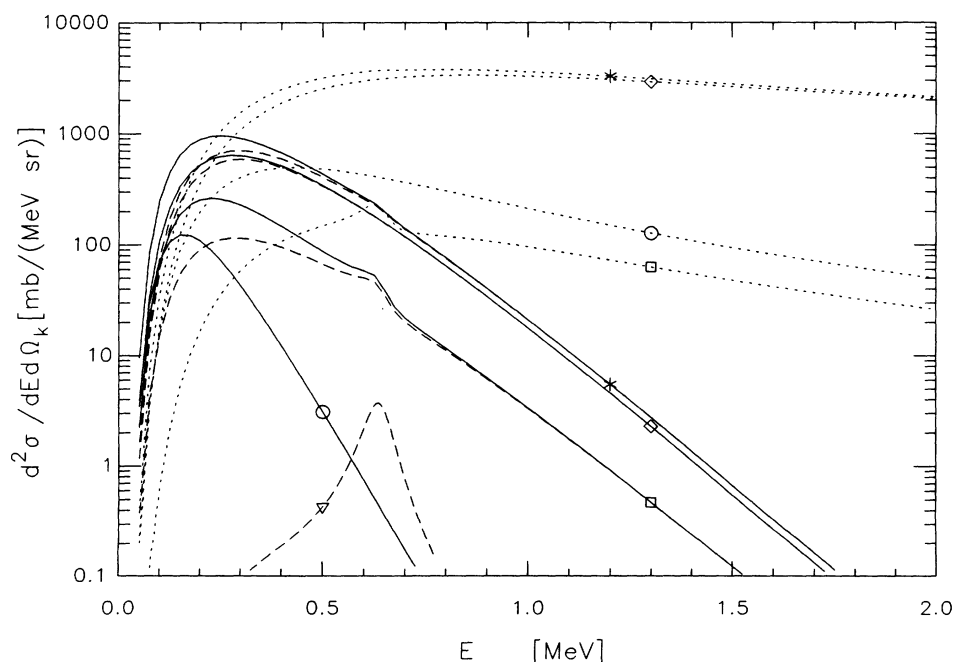


FIG. 5. Breakup cross section of the reaction $^8\text{B} + ^{208}\text{Pb} \rightarrow ^7\text{Be} + p + ^{208}\text{Pb}$ as a function of the relative energy E for a ^8B scattering angle of $\vartheta = 15^\circ$ and a projectile energy of 5 MeV/A. See Fig. 4 for an explanation of the marks.

tion becomes very forward peaked at large beam energies, dominated by the $E1$ one-photon exchange. The increase of the cross section in the peak region at larger projectile energies is evident as well as the decrease of the width of the peak. Simultaneously, the ratio of $E2$ to $E1$ contributions in the first-order results gets smaller and the $M1$ to $E1$ ratio increases. (The $M1$ contribution in Fig. 6(a) is too small to be shown.) The angular dependence reflects

directly the impact parameter dependence, which in turn is a measure of the strength and adiabaticity parameters [χ and $\xi(\vartheta)$]. For small angles, corresponding to large impact parameters, the strength parameter is low, and first-order effects dominate. The first-order contributions scale approximately like ϑ^{-2} ($E1$, $M1$) and ϑ^0 ($E2$). For too large impact parameters, i.e., $\vartheta < \vartheta_{\min}$, the collision becomes adiabatic and the excitation cross section

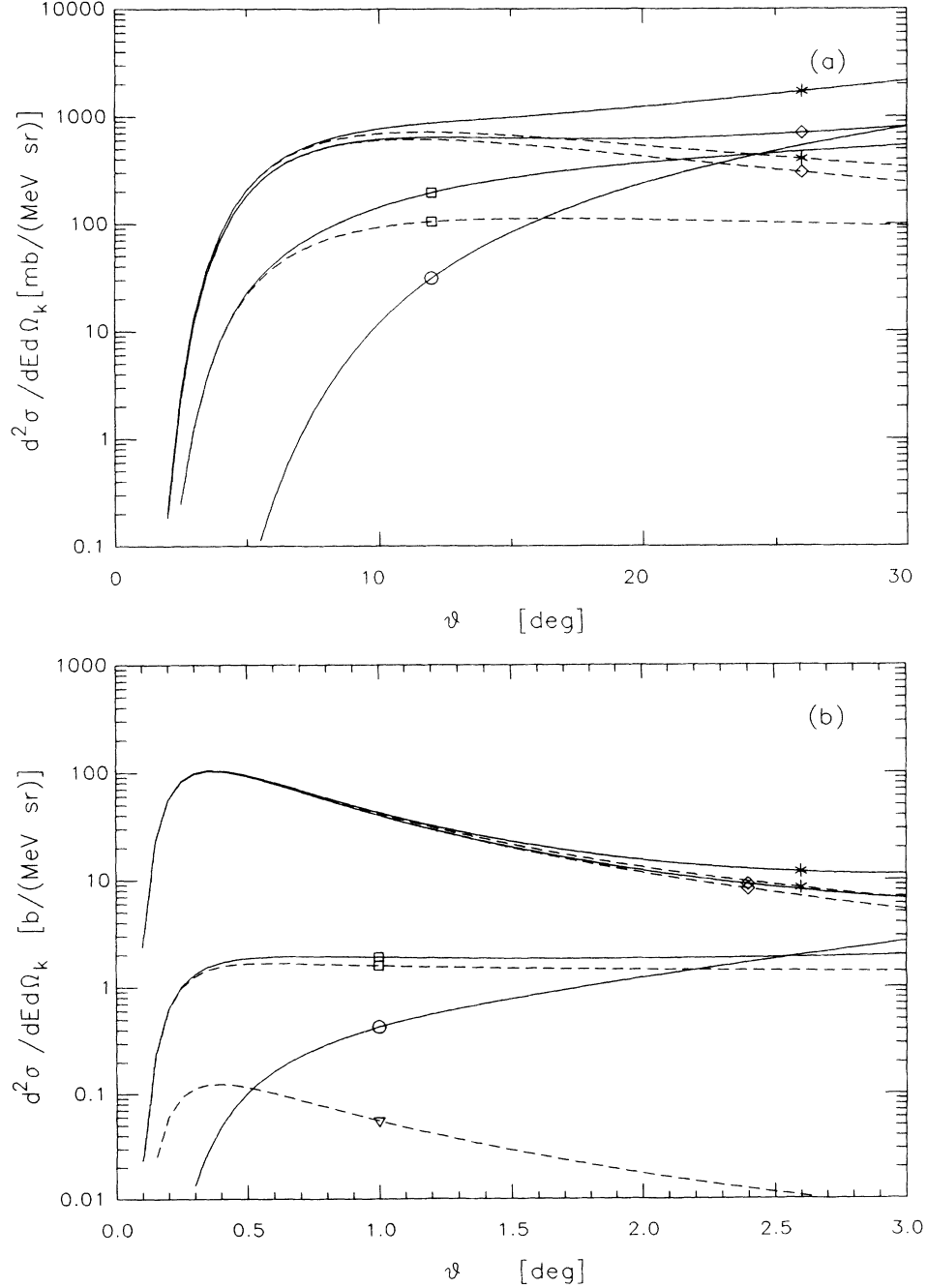


FIG. 6. Breakup cross section of the reaction ${}^8\text{B} + {}^{208}\text{Pb} \rightarrow {}^7\text{Be} + p + {}^{208}\text{Pb}$ as a function of the ${}^8\text{B}$ scattering angle ϑ at the relative energy $E = 250$ keV and a projectile energy of (a) 5 MeV/A, (b) 46.5 MeV/A, and (c) 200 MeV/A. See Fig. 4 for an explanation of the marks.

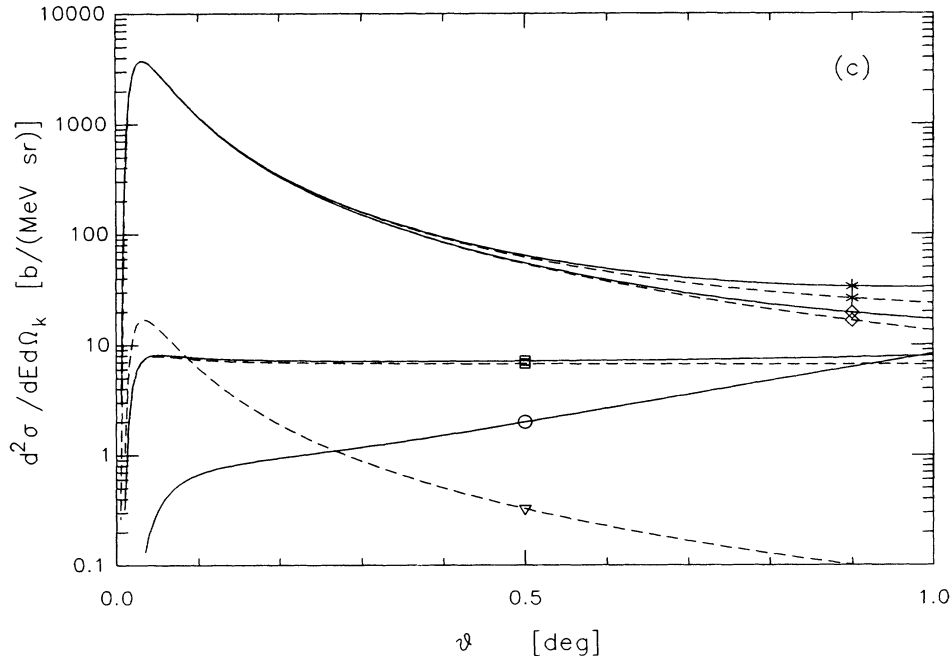


FIG. 6. (Continued).

vanishes exponentially. As is expected, these qualitative considerations can be clearly seen in our model calculations. Higher-order effects show up at increasing angles as the second-order contributions behave like ϑ^0 ($E1E1$), ϑ^2 ($E1E2$), and ϑ^4 ($E2E2$). For the extraction of the astrophysical S factor ($E1$ only) forward angles are favorable. Of course, measurements at larger angles would assure us that the description of the process is well understood theoretically.

Higher-order effects can also change the angular correlation of the fragments because of the strong sensitivity due to interference effects. The angular distribution of the proton is shown in Fig. 7 for a constant impact parameter of $b = 50$ fm. The first-order calculation yields an almost isotropic emission if only the electric dipole excitation is taken into account because breakup into the s wave dominates. The interference effect of first-order $E1$ and $E2$ contributions distinctly changes the angular distribution. Deviations caused by second-order effects are more important at small projectile velocities. But “post-acceleration” effects, even at sub-Coulomb energies, should be controllable. An experimental study of the angular correlation, although quite difficult, will be of great use for the theoretical understanding.

V. CONCLUSIONS

Due to the low binding energy of ${}^8\text{B}$, Coulomb dissociation cross sections can become rather large, even at relatively moderate projectile energies. This renders the Coulomb dissociation method potentially useful for the extraction of astrophysical S factors for the ${}^7\text{Be}(p,\gamma){}^8\text{B}$ process. Since this method relies on the one-photon

exchange approximation higher-order effects have to be carefully investigated. In the low- ξ limit, this was shown to be possible by using closure. In addition to the usual electromagnetic matrix elements, which enter into the model-independent approach of first-order Coulomb excitation, new types of matrix elements appear. Some of them are related to electric matrix elements of higher multipolarity. We evaluate them in our exploratory calculation by a simple, realistic model. But this model dependence means no restriction in the statements with respect to the general behavior of the higher-order effects.

Our detailed numerical calculations show the expected trends: dominance of one-photon exchange processes for very peripheral collisions, i.e., small scattering angles. The $E1$ excitation shows a typical ϑ^{-2} behavior, down to a minimum angle ϑ_{\min} , which is determined by the adiabaticity condition. With increasing scattering angle, higher-order and also direct $E2$ contributions increase in importance. As is also expected, higher-order contributions decrease with increasing ${}^8\text{B}$ beam energy. We note that these second-order effects also include the so-called post-acceleration effects. We find them very small at the higher energies, thus one can justly say that these effects are well under control. They will show up at larger angles in sub-Coulomb ${}^8\text{B}$ breakup.

The ${}^8\text{B}$ nucleus deserves a better theoretical treatment to give really quantitative results. A modification of the first-order $E2$ contribution in other nuclear models as compared to our model will directly lead to a corresponding change in the second-order effects from the $E1E1$ coupling. Coulomb dissociation experiments with the ${}^8\text{B}$ nucleus make it even possible to determine the $E2$ contribution to the cross section because of the strong enhancement as compared to the $E1$ contribution.

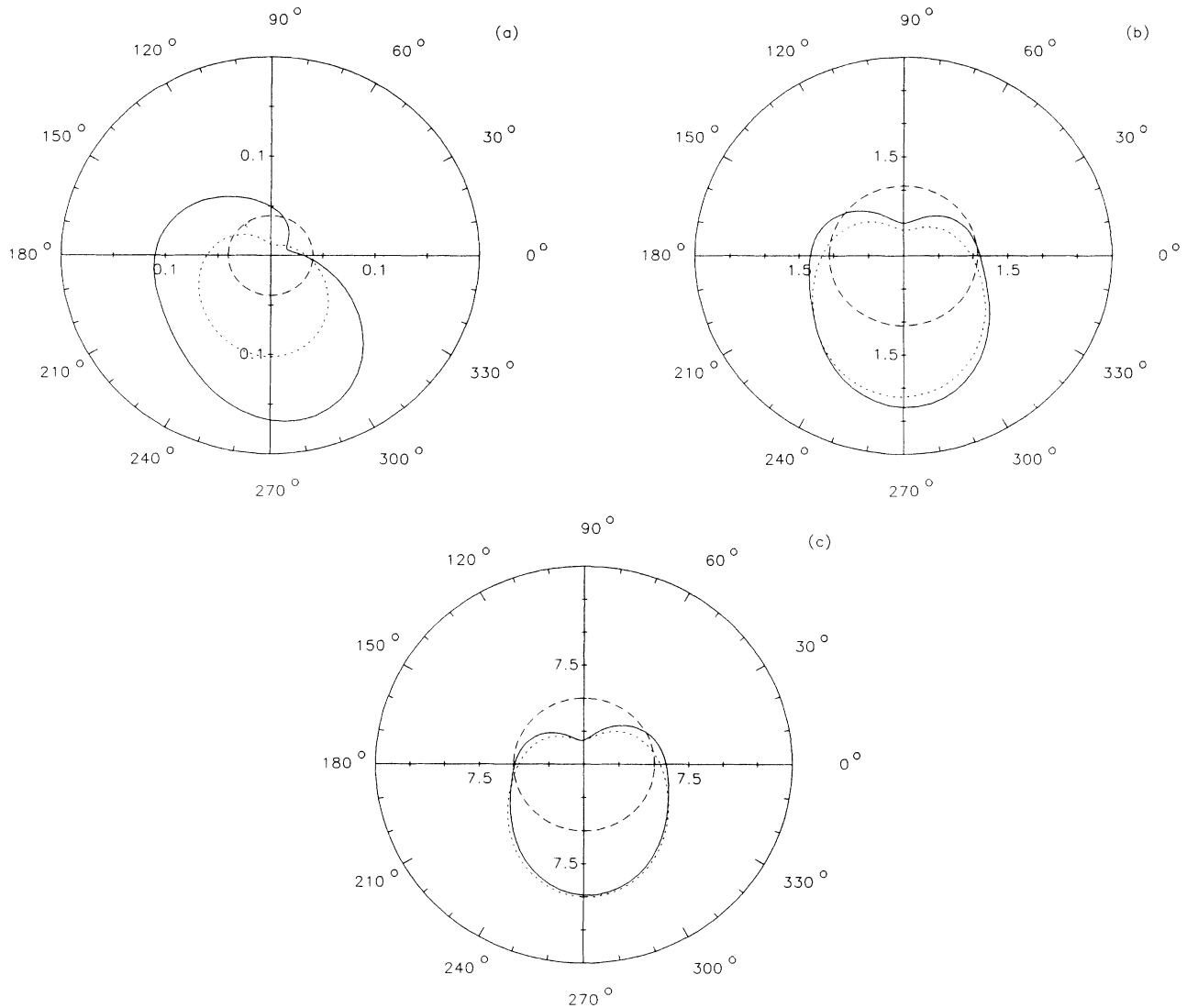


FIG. 7. Angular distribution of the proton in the reaction plane for an impact parameter $b = 50$ fm, a relative energy $E = 250$ keV, and a projectile energy of (a) 5 MeV/A, (b) 46.5 MeV/A, and (c) 200 MeV/A. Results of first order $E1$ (dashed line), first order $E1 + E2 + M1$ (dotted line), first + second order calculation (solid line) in $b/(\text{MeV sr}^2)$. Upper half plane: θ_p , lower half plane: $360^\circ - \theta_p$.

In a recent paper [5] it was shown that nuclear excitation effects are very small. We conclude that a systematic experimental investigation of ^8B Coulomb dissociation will be a useful method to extract the astrophysical S factor for the $^7\text{Be}(p,\gamma)^8\text{B}$ capture reaction. We hope that our investigation stimulates the planning of experiments and leads to an optimal selection of the experimental conditions. We further hope that the present paper provides a theoretical framework for an analysis which can be done as model-independently as possible. The consistency of the data with the theoretical analysis will

hopefully convince us of the reliability of the extracted S factors.

ACKNOWLEDGMENTS

We are very grateful to P. Aguer, C. A. Bertulani, M. Gai, J. Kiener, K. Langanke, T. Motobayashi, H. Rebel, and H. Utsunomiya for discussions, correspondence, and encouragement.

- [1] G. Baur, C. A. Bertulani, and H. Rebel, Nucl. Phys. **A458**, 188 (1986).
- [2] G. Baur and H. Rebel, J. Phys. G **20**, 1 (1994).
- [3] J. N. Bahcall, *Neutrino Astrophysics* (Cambridge University Press, New York, 1989).
- [4] T. Motobayashi, N. Iwasa, Y. Ando, M. Kurokawa, H. Murakami, J. Ruan (Gen), S. Shimoura, S. Shirato, N. Inabe, M. Ishihara, T. Kubo, Y. Watanabe, M. Gai, R. H. France III, K. I. Hahn, Z. Zhao, T. Nakamura, T. Teranishi, Y. Futami, K. Furutaka, and Th. Delbar, submitted to Phys. Rev. Lett.
- [5] C. A. Bertulani, Phys. Rev. C **49**, 2688 (1994).
- [6] K. Langanke and T. D. Shoppa, Phys. Rev. C **49**, R1771 (1994); Erratum submitted to Phys. Rev. C.
- [7] C. A. Bertulani (private communication).
- [8] T. Motobayashi (private communication).
- [9] S. Typel and G. Baur, Phys. Rev. C **49**, 379 (1994).
- [10] S. Typel and G. Baur, Nucl. Phys. **A573**, 486 (1994).
- [11] G. F. Bertsch and C. A. Bertulani, Nucl. Phys. **A556**, 136 (1993).
- [12] C. A. Bertulani and G. F. Bertsch, Phys. Rev. C **49**, 2839 (1994).
- [13] L. F. Canto, R. Donangelo, A. Romanelli, and H. Schulz, Phys. Lett. B **318**, 415 (1993).
- [14] G. Baur and M. Weber, Nucl. Phys. **A504**, 352 (1989).
- [15] A. N. F. Aleixo and C. A. Bertulani, Nucl. Phys. **A505**, 448 (1989).
- [16] F. C. Barker, Aust. J. Phys. **33**, 177 (1980).
- [17] K. H. Kim, M. H. Park, and B. T. Kim, Phys. Rev. C **35**, 363 (1987).
- [18] C. W. Johnson, E. Kolbe, S. E. Koonin, and K. Langanke, Astrophys. J. **392**, 320 (1992).
- [19] H. Krauss, K. Grün, T. Rauscher, and H. Oberhummer, Ann. Phys. **2**, 258 (1993).
- [20] P. Descouvemont and D. Baye, Nucl. Phys. **A567**, 341 (1994).
- [21] F. Ajzenberg-Selove, Nucl. Phys. **A490**, 1 (1988).
- [22] M. Gai and T. Motobayashi (private communication).
- [23] G. Baur, F. Rösler, D. Trautmann, and R. Shyam, Phys. Rep. **111**, 333 (1984).
- [24] P. D. Parker, Phys. Rev. **150**, 851 (1966).
- [25] R. W. Kavanagh, T. A. Tombrello, J. M. Mosher, and D. R. Goosman, Bull. Am. Phys. Soc. **14**, 1209 (1969).
- [26] B. W. Filippone, A. J. Elwyn, C. N. Davids, and D. D. Koetke, Phys. Rev. Lett. **50**, 412 (1983); Phys. Rev. C **28**, 2222 (1983).